Chapter 1
Responses of Insect Olfactory Neurons to Single Pheromone Molecules

Karl-Ernst Kaissling

Abstract The status of our understanding of the molecular processes underlying olfactory reception in insects was summarized by Wicher (Progress in molecular biology and translational science, vol 130. Elsevier, New York, pp 37–54, 2015; see also Chap. 4) and recently by Stengl (Chemosensory transduction in arthropods. In: Byrne JH (ed) Oxford handbooks online. The Oxford handbook of invertebrate neurobiology. Oxford University Press, pp 1–42. https://doi.org/10.1093/oxfordhb/9780190456757.013.15, 2017) and Wicher and Grosse-Wilde (Chemoreceptors in evolution. In: Kaas J (ed) *Evolution of nervous systems 2e*. Elsevier, Oxford, pp 245 -255, 2017). The present chapter adds an overdue review of studies dealing with the responses of moth antennal olfactory neurons (nerve cells) to single impacts of airborne pheromone molecules. Weak pheromone stimuli elicit "elementary receptor potentials" (ERPs) which consist of one or several "bumps", transient negative deflections of the resting trans-epithelial potential recorded from the tips of single trichoid sensilla, i.e. olfactory mini-organs on insect antennae. In the male silkmoth *Bombyx mori* a bump may elicit one, seldom two or three nerve impulses, but up to five impulses in the sphingid moth *Manduca sexta*. According to behavioral, electrophysiological and radiometric studies, the ERPs are elicited by single pheromone molecules. The analysis of the neuro-electrical circuit of moths sensilla revealed that the average bump amplitude (of about 0.5 mV) reflects an increase of the membrane conductance of an olfactory neuron by about 30 pS. The observation of several sublevels of bump amplitudes in *B. mori* suggest either varying degrees of opening of a single ion channel or varying numbers of superimposed openings of smaller channels. At weak stimulus intensities ion channels might be directly gated by the odor molecule-receptor interaction. At higher intensities intracellular signaling might be responsible for diminished channel opening that causes widening the range of the pheromone dose-response and adaptation (reduced responsiveness) after strong stimuli. In *B. mori* the temporal characteristics of the responses to single pheromone molecules were used to calculate the

K.-E. Kaissling (✉)
Max-Planck-Institut Seewiesen, Starnberg, Germany
e-mail: kaissling@orn.mpg.de

J.-F. Picimbon (ed.), *Olfactory Concepts of Insect Control - Alternative to Insecticides*, https://doi.org/10.1007/978-3-030-05165-5_1

apparent residence time of the pheromone molecule at the receptor molecule, in the range of 100 ms.

1 Introduction

Insects as well as vertebrates perceive olfactory stimuli by means of so-called primary sensory cells or receptor neurons that have an apical (dendritic) portion sensitive to odor molecules, and a basal axon transmitting nerve impulses (action potentials) to the brain and the insect central nervous system, respectively. Via olfactory receptor molecules the odor stimulus is transduced into a change of the electrical membrane conductance of the dendrite. This occurs in the olfactory epithelium inside the nasal cavity of vertebrates and at the level of sensory organs such as the antennae of insects. The associated electrical *depolarization* of the membrane potential (so-called receptor *potential*) elicits nerve impulses within an intermediate generator region around the cell soma of the sensory nerve cell or receptor neuron.

In insects a few olfactory receptor neurons together with auxiliary cells are enclosed in cuticular structures and form a sensory mini-organ called sensillum. A typical hair-like sensillum trichodeum is schematically shown in Fig. 1.1 (bottom). Numbers of sensilla are distributed on insect antennae, pairs of head appendages serving as composite sense organs (Fig. 1.1, top). They bear sensilla for olfactory stimuli including carbon dioxide, but also for stimuli of other sensory modalities such as taste, mechanoreception, or temperature (Keil 1999). Some antennae, e.g. those of some male moths are particularly designed as sieves for efficiently catching air-borne odorant molecules such as sexual pheromones released by the female moths over large distances. The comb-like antennae of these moths species (Fig. 1.1, top) are laced with numerous olfactory sensilla trichodea, with hair lenghts of up to 500 µm (Keil 1984, 1989).

The odorant/pheromone molecules caught by the hairs penetrate the hair wall via numerous pores. Inside the hair the water-insoluble odorant molecules reach the neuronal dendrites, while carried by the abundant odorant binding proteins (OBPs), dissolved in the sensillum lymph (Vogt and Riddiford 1981; Vogt et al. 1985). Finally the odorant molecules interact with receptor molecules of the dendritic plasma membrane, probably while still bound to the binding protein (Kaissling 2009b), and with the help of the sensory neuron membrane protein (SNMP1) found by Rogers et al. (1997, 2001). SNMP is a homolog of the CD36 protein family and is a signaling component necessary for odorant sensitivity (Jin et al. 2008; Li et al. 2014).

This review concentrates on the interaction of odorants and receptor molecules and the following processes: the changes of neuronal membrane conductance and associated receptor potentials. Influencing factors, such as stimulus intensity, temperature, and various agents modulating the responses will be discussed (see also Chap. 4). The focus of this review is directed to the responses to single odor/phero-

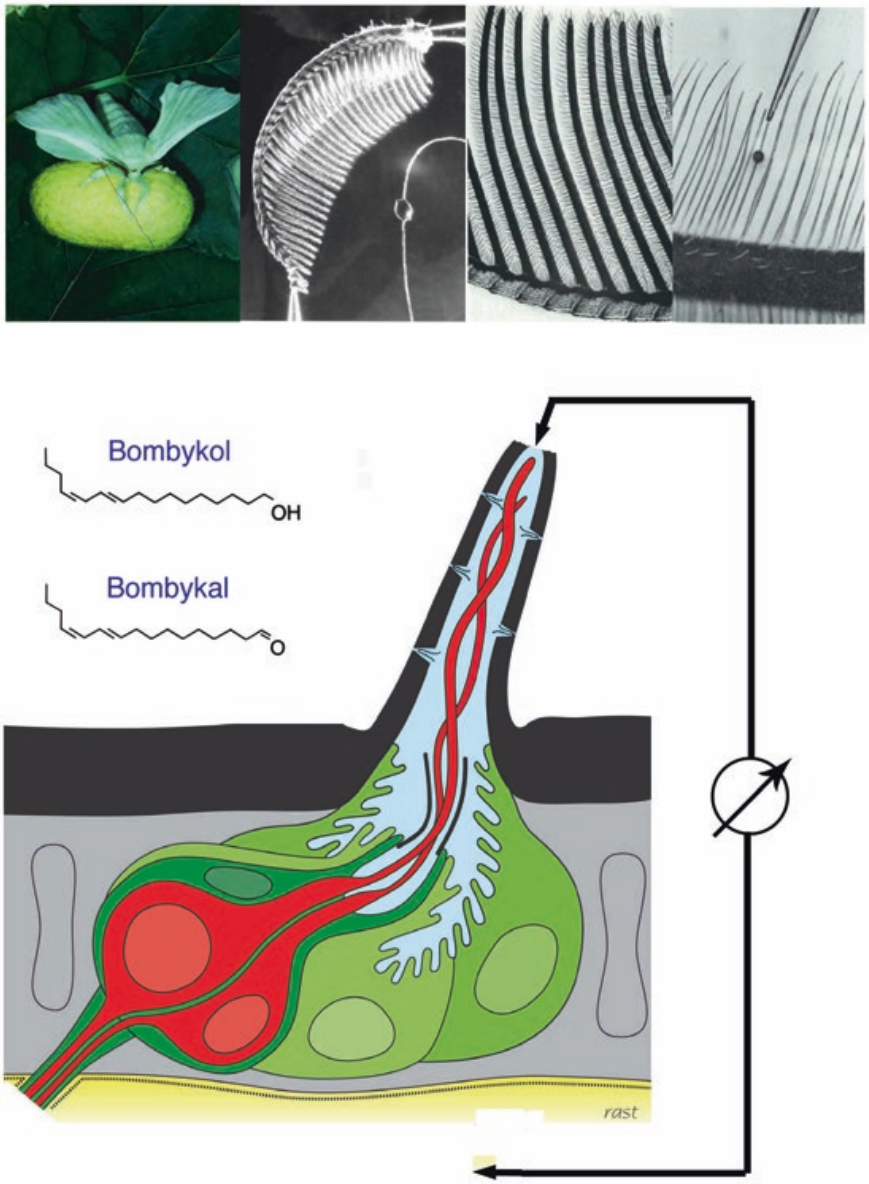

Fig. 1.1 Moth antennae with olfactory sensilla. From left to right, *Bombyx mori:* male moth with cocoon – isolated antenna with electrode capillaries for electroantennogram recording and thermistor for measuring airstream velocity or temperature – antennal branches with sensilla trichodea (hair length 100 µm, by courtesy of R. A. Steinbrecht) – *Antheraea polyphemus:* antennal branch with sensilla trichodea (hair length 300 µm), with recording electrode capillary slipped over one hair after its tip was severed. Mouth of a capillary for local stimulation of the hair – Bottom: Scheme of a sensillum trichodeum with two receptor neurons (coloured red) surrounded by three auxiliary cells (by courtesy of R. A. Steinbrecht). Arrows show the position of electrodes for recording transepithelial potentials or currents. Sensillum lymph within the hair lumen (coloured blue) containing odorant binding protein (OBP) or pheromone binding protein (PBP). In each sensillum trichodeum of male *B. mori* one neuron responds to bombykol (sexual attractant), the other one to bombykal (behavioral inhibitor)

mone molecules. These responses observed in moths are compared with respective responses of olfactory receptor neurons in vertebrates.

2 The Olfactory Threshold of Moths

Combined radiometric, morphological, electrophysiological and behavioral investigations (Kaissling and Priesner 1970; Kaissling 2009a, 2014) were employed in order to study the absolute olfactory sensitivity of the silkmoth *Bombyx mori.* This became possible after the discovery of the very first pheromone chemical in the silkmoth (Butenandt et al. 1959). The compound was named Bombykol after the Latin name for the silkworm moth (*Bombyx mori*). Bombykol is the only signal chemical used by female silk moth to attract a conspecific male. This made *B. mori* a model of choice for studying the simplest possible pheromone system.

Tritium-labeled pheromones such as ^{3}H-*(E,Z)*-10,12-hexadecadienol (bombykol) from *B. mori* (Kasang 1968) but also ^{3}H-*(E,Z)*-6,11 hexadecadienyl acetate from the two giant saturniid moths *Antheraea polyphemus* and *Antheraea pernyi* (Kasang et al. 1989a, b) served as important tools for quantitative studies in this process. The ^{3}H-labeled compounds enabled us to measure (i) their amounts loaded on the experimental odor source (down to 10^{-7} µg on a 1 cm^2 filter paper, fp), (ii) the number of stimulus molecules released from the odor source (Kaissling and Priesner 1970; Kaissling 1995), (iii) the fraction adsorbed by the insect antenna, (iv) the fraction (80%) of adsorbed molecules caught by the long antennal hairs (sensilla trichodea) (Steinbrecht and Kasang 1972; Kanaujia and Kaissling 1985), and finally (v) the fraction of adsorbed molecules entering the hair lumen (>50%).

Fifty percent of male silkmoths *B. mori* responded with wing fluttering to a source load of about 2×10^{-5} µg of the main pheromone component bombykol (BOL), i.e. a concentration of about 3000 stimulus molecules per ml of air applied during one s at an air stream velocity of 60 cm/s. With this load and upon a 1-s stimulus about 24% of the 17,000 antennal hairs received a bombykol molecule, and about 6% of the 17,000 BOL-neurons fired a nerve impulse (Kaissling and Priesner 1970, reviewed in Kaissling 1971, 2014). A 1-s stimulus with a load of 3×10^{-4} µg of bombykol per fp elicited on the average one nerve impulse per olfactory neuron of *B. mori.* At loads below 10^{-3} µg the nerve impulses occurred at random (Poisson) distribution. From these investigations we concluded that one bombykol molecule is sufficient to elicit a nerve impulse.

Electrophysiological recordings from pheromone receptor neurons and also from secondary neurons within the deutocerebrum of the central nervous system (see Chaps. 2 and 3) suggest that the two above-mentioned saturniid species are even more sensitive to their pheromones than the silk moth *B. mori*. Loads of 10^{-5} µg/fp of the main pheromone components *(E,Z)*-6,11-hexadecadienyl acetate and *(E,Z)*-6,11-hexadecadienal produced one or a few impulses in *A. polyphemus* and *A. pernyi,* respectively (Boeckh and Boeckh 1979). Besides somewhat different experimental conditions the responses to loads 30-fold smaller than needed in *B. mori* must be due

to the much longer hair sensilla of the male saturniid moths (400 µm instead of 100 µm in *B. mori*) (Keil 1984), and due to their different arrangement on the antennal branches providing a higher efficiency of catching molecules. The deutocerebrum neurons responded to pheromone loads as low as 10^{-7} µg/fp indicating the expected massive convergence of sensory to central neurons (at least 100:1) (ibid.).

Here we include responses of the olfactory receptor neurons tuned to *(E,Z)*-10,12-hexadecadienal (bombykal, BAL), a secondary component in the sex pheromone of *B. mori* (Kaissling et al. 1978). A pair of BOL- and BAL-neurons innervates each sensillum trichodeum of the male antenna (see Fig. 1.1). Each type of neuron also responds to the other pheromone component but only at 10,000-fold stronger stimulus loads, respectively, demonstrating the remarkable odor-specificity of pheromone receptor neurons in moths. While bombykol alone elicits the entire mating behavior of the male moth, bombykal acts as a behavioral inhibitor (ibid.). Bombykal applied at the same loads on fp as bombykol produced somewhat higher nerve impulse numbers in the BAL-neuron, respectively, presumably due to a higher release of the aldehyde from the fp source.

It should be mentioned that bombykal is also a pheromone component in Sphinx moths, including *M. sexta* (Starrat et al. 1979). In this species bombykal elicited a few nerve impulses with loads of 10^{-5} µg/fp and stimuli of 50 ms only (Fig. 5 in Dolzer et al. 2003). Although not mentioned by the authors, these data strongly suggest that nerve impulses are elicited by single pheromone molecules not only in *Bombyx* but also in Sphinx moths.

3 ERPs and Bumps

At low stimulus intensities (below 10^{-3} µg per odor source), only a few nerve impulses per neuron and per s are fired. These impulses are preceeded and thought to be elicited by so-called "elementary receptor potentials" or ERPs (Kaissling 1974; Kaissling and Thorson 1980). The ERP appears as a transient depolarization ("bump") preceding one or a few nerve impulses (Fig. 1.2a, b, d, and i), or as a group of bumps (Fig. 1.2c, d, and i). As discussed below, an ERP showing a group of bumps may originate from repetitive activations of an individual receptor molecule by a single pheromone molecule.

In trans-epithelial recordings from BAL-neurons, the ERPs showed bump amplitudes in the range of 0.5 mV, a bump duration of 10.2 ms (925 bumps), and an average bump-group (burst) duration of 118 ms (452 bursts) (cell A in Minor and Kaissling 2003). The shape of ERP-bumps is determined by the capacitances of the electrical sensillum circuit and depends on temperature (ibid.) (Fig. 1.2h), according to the temperature dependence of plasma membrane resistances (De Kramer 1985; Kodadová and Kaissling 1996). Interestingly, BOL- and BAL-neurons in *B. mori* produce bumps differing in the steepness of bump onset and average latency between bump onset and nerve impulse, about 20 ms and 10 ms for the BOL- and BAL-neuron, respectively (Fig. 1.2b). At least 5 ms after its onset, a bump may

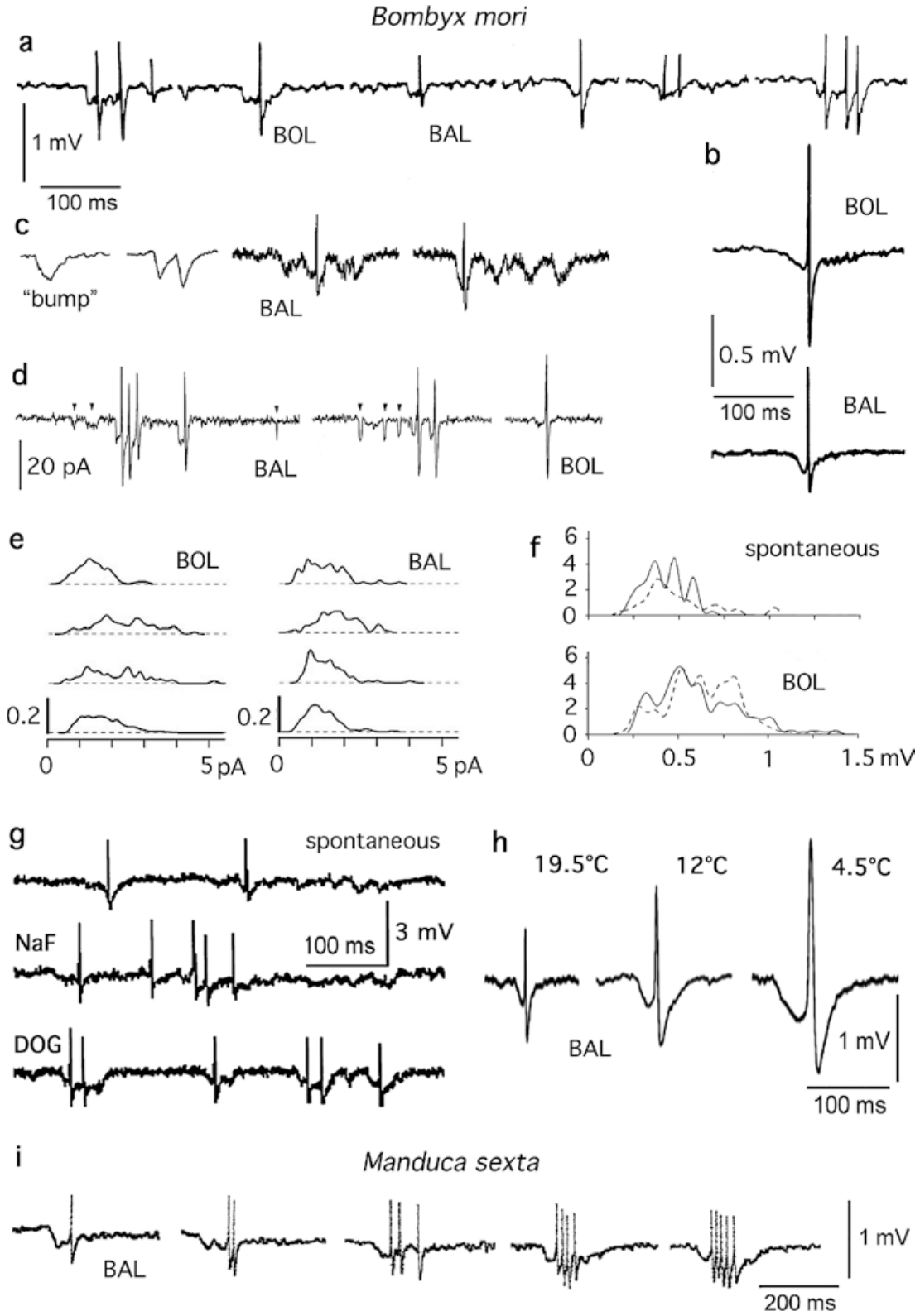

Fig. 1.2 Responses to single molecules of bombykol (BOL) and bombykal (BAL), transepithelial DC-recordings between tips of antennal sensilla trichodea and the hemolymph space. (**a**–**h**) Male *B. mori*: (**a**) Selected "bumps"associated with large nerve impulses (BOL-neuron) or small impulses (BAL-neuron). (**b**) Averages of 50 such events from each neuron type, respectively, added by using the first nerve impulse as a trigger (Kaissling and Thorson 1980). (**c**) Elementary

elicit only one nerve impulse, seldom two or three impulses in the silkmoth (Fig. 1.2a, d); in contrast, up to five impulses per bump were observed in BAL-sensitive neurons in the sphingid moth (Fig. 1.2i).

With weak stimuli eliciting only a few nerve impulses/s the ERPs appear randomly distributed (Fig. 1.3a), as expected for the random arrival of stimulus molecules. Adding up the DC-recorded traces obtained by many such stimuli results in a fluctuating time course similar to the response generated by a single but stronger stimulus (Fig. 1.3b). The fluctuations are even better visible, if the nerve impulses are selectively blocked, e.g. by the insecticide permethrin (Fig. 1.4), known to block the generation of nerve impulses (Vijverberg et al. 1982). This drug does not affect the production of the receptor potential including the ERPs (Kaissling 1980).

4 Electrical Circuit Analysis

For a better understanding of bump generation, the electrical properties of the insect olfactory sensillum were studied using extracellular (trans-epithelial) recordings (see Fig. 1.1, bottom). Following the pioneering analysis of the electrical circuit of insect mechanoreceptive sensilla (Thurm and Küppers 1980), several studies dealt with the insect olfactory sensillum (Zack 1979; Kaissling and Thorson 1980; De Kramer 1985; Redkozubov 1995, 2000a; Kodadová and Kaissling 1996; Vermeulen and Rospars 2001; Minor and Kaissling 2003). Transepithelial tip recordings with one electrode at the opened hair tip (Kaissling 1974, 1995) and the other within the hemolymph space (see Fig. 1.1, bottom) offer conditions similar to whole cell patch clamp recordings. As it were the resting transepithelial resistance between the two extracellular electrodes (406, 214, and 143 MOhm, at 8, 18, and 28 °C, respectively, from Table 1 in Kodadová and Kaissling 1996) corresponds to the sealing resistance ("Gigaseal") in loose patch clamp recordings (Stühmer et al. 1985). This transepithelial resistance is due to the apical membranes of the three auxiliary cells that surround the receptor neurons at the

Fig. 1.2 (continued) receptor potentials (ERPs) with one to four bumps, recorded from the same BAL-neuron as shown in Fig. 1.3. (**d**) Elementary receptor currents (ERCs), tip-recording under voltage clamp. Bumps with and without (marked) nerve impulses. (**e**) Amplitude distributions of ERC-bumps eliciting one nerve impulse each, from selected BOL- and BAL-neurons, respectively, upon weak pheromone stimulation. Ordinate: Rel. probability of events/bins of 0.1 pA (d and e from Redkozubov 2000a). (**f**) Amplitude distributions of spontaneous (above) and BOL-induced ERP-bumps (below) eliciting one nerve impulse each. The two curves of each diagram are averages from 6 (solid lines) and 7 (broken lines) BOL-neurons, with n = 246 and 178 spontaneous, and n = 520 and 557 BOL-induced bumps, respectively. Ordinates: average number of events/bins of 0.05 mV. (**g**) First trace: Spontaneous activity. Second trace: 20 mM NaF, applied via tip electrode. Third trace: 0.1 mM DOG (f and g from Pophof and Van der Goes van Naters 2002). Nerve impulses from BOL-neuron. (**h**) Single bumps + nerve impulses from a BAL neuron at different temperatures (Minor and Kaissling 2003). (**i**) Male *M. sexta:* ERPs with nerve impulses after weak BAL-stimuli (Kaissling 2013). In two neurons we counted 37 and 40 bumps with 0–7 impulses and found averages ± sd of 2.6 ± 2.0, and 2.1 ± 1.7 impulses per bump, respectively (unpublished observations)

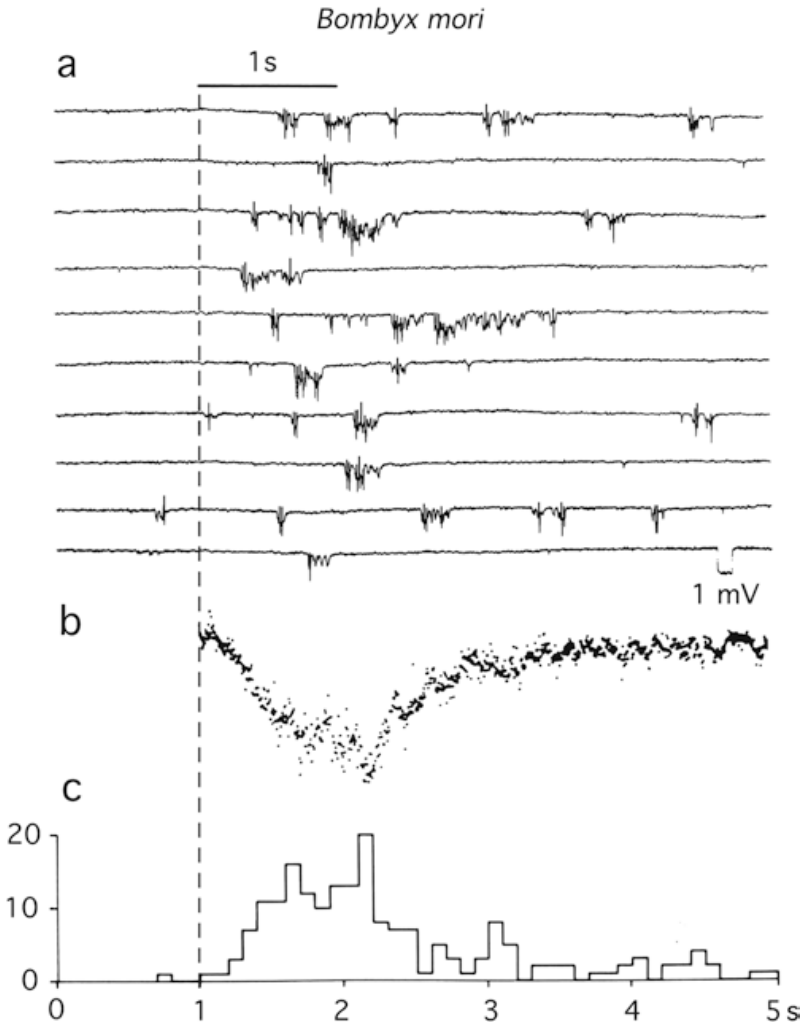

Fig. 1.3 Elementary receptor potentials (ERPs) and nerve impulses DC-recorded from one sensillum trichodeum of a male *B. mori*. (**a**) Ten consecutive responses to 1 s stimuli of bombykal (1 ng/filter paper) with 1 min intervals between stimuli. Single and superimposed ERPs. (**b**) 30 consecutive traces as shown in (**a**) were added. (**c**) Numbers of nerve impulses in 100 ms bins were summed from the 30 responses. The average number of nerve impulses during 5 s was 6.4 per stimulus, their average reaction time was around 600 ms. Same mV calibration for a and b, same time axis for **a**–**c** (**a**: Kaissling 1986; **a**–**c**: Kaissling 1987)

sensillum base (see Fig. 1.1, bottom). In the resting state the parallel current path across the dendrites of the receptor neurons inside the hair has a much higher resistance, in the gigaohm range (6.6 GOhm, Redkozubov 1995); it represents the "patch" resistance, which decreases upon odor stimulation. This arrangement of resistances from sensory and auxiliary cells allows to detect stimulus-induced electrical changes of the neuronal dendrite membrane as conveniently as with intracellular recordings.

Under these conditions, the receptor potentials and the nerve impulses are picked up with opposite polarity (Thurm and Küppers 1980; De Kramer et al. 1984). The receptor potentials appear as negative deflections (i.e. *changes* of the transepithelial

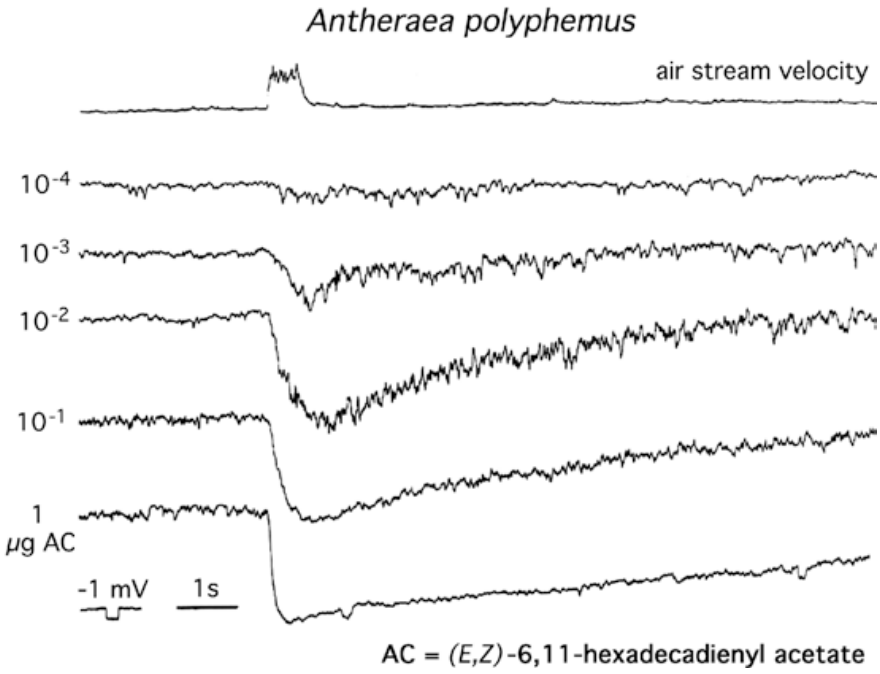

Fig. 1.4 Receptor potentials recorded from *A. polyphemus* upon 500 ms stimuli at increasing loads of the pheromone source (µg per filter paper). The nerve impulses were blocked by treatment with the insecticide (+)-trans-permethrin (Kaissling 1980)

potential), while the nerve impulses elicited within the soma region (the cell body) of the neuron start with a positive phase. The separate functions of dendrite and soma were confirmed using local adaptation (reduced responsiveness) of receptor neurons by pheromone stimuli restricted to a small section of the olfactory hair (see Fig. 1.1, top) (Zack 1979; Zack-Strausfeld and Kaissling 1986), by local anaesthesis (Stange and Kaissling 1995), and by selective cooling of the olfactory hair with the neuronal dendrites (Kodadová and Kaissling 1996).

Moth pheromone sensilla show a resting transepithelial potential (of about +40 mV, Zack 1979). This is due to a special voltage source located in the folded apical membrane of the auxiliary cells (see Fig. 1.1, bottom) common for insect sensilla (Thurm and Küppers 1980). The receptor potentials (i.e. the potential *changes*) amount up to −30 mV upon pheromone stimulation, while trans-epithelial resistances may be reduced by up to 25% (Zack 1979; Kodadová and Kaissling 1996). The circuit analysis revealed that a bump could be generated by a conductance increase of the neuronal membrane inside the hair lumen in the range of 30 pS (Kaissling and Thorson 1980).

A conductance increase of 30 pS could be produced by opening a single ion channel, such as known from the motor endplate, opened by acetylcholine (Neher and Sakmann 1976). Thus, a bump of the olfactory neuron could well indicate opening of a single ion channel. This would suggest that the ERP, the first cellular response to a single stimulus molecule, is a purely electrical phenomenon, not

requiring amplification via intracellular metabolic mechanisms similar to those involved in vertebrate olfactory transduction (Kaupp 2010).

The depolarization of the neuronal membrane is passively conducted from the hair towards the soma region. According to the electrical sensillum model (Kaissling 1987), the depolarisation of the soma membrane during a bump is little higher than the trans-epithelially recorded bump amplitude, in the range of 0.5 mV, obviously large enough to trigger nerve impulses at the neuron soma. Experimentally applied voltage- or current-stimuli elicit nerve impulses, but never bumps (Redkozubov 1995).

Later studies showed a significant variability of bump amplitudes, even in spontaneous bumps. Using trans-epithelial voltage clamp Redkozubov (2000a) recorded elementary receptor currents (ERCs, equivalent to ERPs in voltage recordings) from 14 BOL- and 11 BAL-neurons. The amplitudes of ERC-bumps eliciting one nerve impulse each varied from <1 to 5 pA in both types of pheromone receptor neurons. For each neuron the distribution of amplitudes was different, often exhibiting several peaks (see Fig. 1.2e). Individual neurons appeared to have bump amplitudes with several (3–5) sublevels of an average size of 0.7 pA as determined for six of the BOL-neurons, and of about 0.6 pA for seven of the BAL-neurons (Redkozubov 2000a).

Corresponding variability of ERPs was reported by Pophof and Van der Goes van Naters (2002) from trans-epithelial voltage recordings where pheromone-elicited bumps had average amplitudes of 0.60 mV in 13 BOL-neurons and 0.55 mV in 8 BAL-neurons. The bump amplitudes varied between 0.2 and 1.5 mV and also showed distributions with several peaks (see Fig. 1.2f). Variation of bump amplitudes in individual neurons might indicate different degrees of opening of a single ion channel or varying numbers of channels opened following the activation of one receptor molecule.

Interestingly, spontaneous bumps eliciting nerve impulses in pure air controls showed smaller amplitudes of 0.45 mV in 13 BOL-neurons (Fig. 1.2f), and 0.51 mV in 9 BAL-neurons (averaged from Table 3 in Pophof and Van der Goes van Naters 2002). The spontaneous firing frequency was 0.157/s for 27 BOL-neurons, and 0.025/s for 20 BAL-neurons (ibid., averaged from Table 2). A spontaneous ERP produced in the absence of pheromone might originate from a spontaneous activation of a single receptor molecule. The apparent rate of spontaneous activations of the bombykol receptor molecule can be obtained from the spontaneous firing rate of the BOL-neuron (0.157/s) divided by the estimated number of receptor molecules per neuron (7.6×10^5, see below). We arrive at spontaneous activations of the bombykol receptor molecule of roughly 2×10^{-7}/s, which is close to the rate of thermal activations of rhodopsin in vertebrate visual cones between 1.34×10^{-7}/s (human) and 5.28×10^{-5}/s (larval tiger salamander, see Ala-Laurila et al. 2004).

The above suggestion of a purely electrical generation of the elementary response is supported by findings of Sato et al. (2008) and Wicher et al. (2008), that the functional insect olfactory receptor is a complex of two or several proteins forming a ligand-gated non-selective cation channel (of 27 pS conductance; Sato et al. 2008; see also Chap. 4). The insect olfactory receptor complex consists of two types of proteins with seven-transmembrane alpha-helical domains, an odorant-specific subunit OR and the co-receptor ORCO, both with a membrane topology with extracel-

lular C-terminus, opposite to the topology of G-protein-coupled olfactory receptors from vertebrates.

The structure of the ORCO unit is extremely conserved in all insect species studied so far (Stengl and Funk 2013). The ORCO-agonist VUAA1 (2-(4-ethyl-5-(pyridin-3-yl)-4H-1,2,4-triazol-3-ylthio)-N-(4-ethylphenyl) acetamide), found by screening over >100,000 compounds) opened channels with 22 pS conductance (1.3 pA at −60 mV holding potential) in outside-out membrane patches of HEK293 cells expressing *Anopheles gambiae* ORCO (Jones et al. 2011). A concentration of 100 μM of VUAA1 applied via the tip electrode to bombykal-sensitive neurons of *M. sexta* increased the spontaneous activity about 20-fold up to about four nerve impulses/s but did not modify the responses to bombykal stimuli. Therefore, and based on previous work, it was concluded that second messengers contribute to the pheromone reception in the Sphingid moths *Manduca sexta* (Nolte et al. 2013, 2016).

Nakagawa et al. (2012) performed site-directed mutagenesis of all 83 conserved Glu, Asp, or Tyr residues in the silkmoth BmOR-1-ORCO pheromone receptor complex and measured functional properties of mutant channels expressed in *Xenopus* oocytes. They provided confirmatory evidence that both subunits contribute to the ion permeability of the insect OR-ORCO complex. First attempts have been made to unravel the precise 3D structure of the OR-ORCO complex (Hopf et al. 2015), but this remains a challenge owing largely to the partially hydrophobic nature of the receptor.

"Spontaneous sensillar potentials" eliciting nerve impulses were recorded from pheromone-sensitive neurons of the Egyptian cotton worm moth *Spodoptera littoralis* (Pézier et al. 2007, 2010). These bump-like events depended on Ca^{2+} concentration within the tip electrode capillary. They occurred especially at low Ca^{2+} concentrations (20 nM) (ibid.), but their occurrence after pheromone stimulation was not assessed. A recent study suggests that transient receptor potential (TRP) like ion channels are involved in moth olfactory transduction (Gawalek and Stengl 2018).

5 Kinetic Model

The temporal characteristics of the ERPs were used to estimate apparent rate constants of the pheromone receptor interaction represented by the following scheme with the receptor molecule R and the ligand FA, i.e. the complex of pheromone F bound to the pheromone binding protein A (see the model of Kaissling 2009b). When a ligand-receptor complex FAR is formed, it may switch one or several times into the excited state FAR′ eliciting one or several bumps of an ERP (or an ERC, respectively):

$$\mathrm{FA} + \mathrm{R} \underset{k_{-5}}{\overset{k_5}{\rightleftharpoons}} \mathrm{FAR} \underset{k_{-6}}{\overset{k_6}{\rightleftharpoons}} \mathrm{FAR}'$$

Assuming that the bumps reflect the activated state FAR′, the apparent rate constants k_6 = 16.8/s, k_{-6} = 98/s, and k_{-5} = 7.7/s were calculated for bombykal neurons of *B. mori* from averages of the duration of bumps (=10.2 ms = $1/k_{-6}$), the durations of gaps between bumps within an ERP (=40.5 ms), and the number of bumps per ERP (=3.2) (Minor and Kaissling 2003).

The rate constants allowed to calculate an apparent life (residence) time *Tc* of the ligand-receptor complex (FAR + FAR´), which was $Tc = (k_6 + k_{-6})/(k_{-5} \times k_{-6})$ = 153 ms for one of the bombykal neurons of *Bombyx mori* (and *Tc* = 135 ms for another bombykal neuron). The model implies that the potential changes caused by opening and closing of one or a few ion channel(s) mirror the activation of a receptor molecule (FAR --> FAR´) and its return (FAR´--> FAR). This would require a tight functional coupling of receptor molecule and ion channel - within a millisecond time interval (Hille 2001) - and would challenge the above idea that one receptor activation opens several ion channels. The kinetic model of Kaissling (2009b) was used to estimate R_{tot} as a fictive total concentration of R within the olfactory hair (volume 2.6 pl) as …

$$R_{tot} = T_c \times U_{sat} \times Q_3 \times \left(k_{-5} + k_6\right) / k_6 = 1.67 \ \ \mu\mathrm{M}$$

… with the pheromone uptake of the hair *Usat* = 30 µM/s, at which the receptor potential is saturated, and with Q_3 = 0.25, the fraction of stimulus molecules adsorbed (at weak stimuli on the hair sensilla) eliciting nerve impulses. The apparent density of receptor molecules within the dendritic membrane of the A-neuron of *A. polyphemus* (426 µm², Keil 1984) amounts to

$$R_{tot} \times N_{\mathrm{Avogadro}} \times \mathrm{hair\ \ volume}\left(2.6\mathrm{pl}\right) / \mathrm{dendritic\ \ area}\left(426\,\mu\mathrm{m}^2\right) = 6100 / \mu\mathrm{m}^2.$$

This number fits to the average density of repetitive structures – putative receptor molecule-ORCO complexes – found by negative staining in isolated membrane vesicles obtained from isolated sensilla of *A. polyphemus.* The density of these structures was about 10,000 units/µm² (Klein and Keil 1984), close to the density of rhodopsin, the photoreceptor molecule in visual cells of the vertebrate retina, with 40,000 units/µm² of the outer disk membrane (Dratz and Hargrave 1983).

The number of receptor molecules per neuron obtained from the above density (6100/µm²) and from the dendritic membrane area (426 µm²) amounts to 2.6×10^6 for the A-neuron of *A. polyphemus* (tuned to *(E,Z)*-6,11 hexadecadienyl acetate), and to 3.8×10^5 for the BOL-neuron of *B. mori,* the latter with a dendritic area of 62 µm² (Gnatzy et al. 1984).

Using the estimated amount of receptor molecules further important numbers may be derived. If every OR-ORCO complex constitutes an ion channel, there

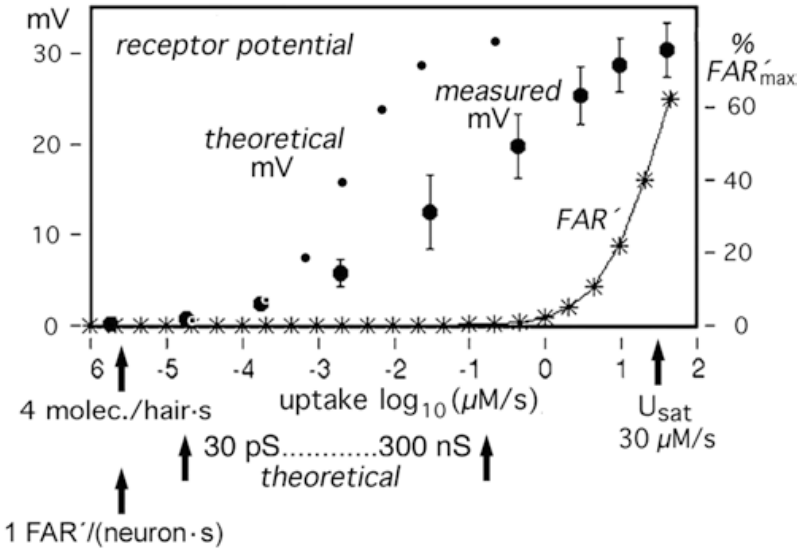

Fig. 1.5 Steady dose–response functions of the theoretical and measured receptor potential (mV), and of FAR′ (% of FAR′max) produced by the kinetic model of Kaissling (2009b). *Abscissa* Stimulus uptake U (molecules adsorbed per second and per hair volume, given in μM/s), calibrated by measuring the release of radioactivity from the sources loaded with the ^{3}H-labeled major pheromone component *(E,Z)*-6,11-hexadecadienyl acetate (Kaissling 1995) and by measuring the adsorption on the antennal hairs of *Antheraea polyphemus* (Kanaujia and Kaissling 1985). The smallest load (dot near −6) was 10^{-5} μg per filter paper, the load for the saturating uptake Usat was 1 mg on a 10-mg piece of cotton. *Large dots* Average amplitudes (±s.d.) of receptor potentials transepithelially recorded from 14 single sensilla trichodea of male moths upon 2s-pheromone stimuli with (Zack 1979). The three lowest values were re-measured by Blanka Pophof, Seewiesen (error bars not visible). *Asterisks* Model equilibrium concentrations of FAR′ (plotted as % of FAR′max) at 2 s after stimulus onset. FAR′ increases linearly with the pheromone uptake over the entire range up to about 10 μM/s (Kaissling 1998). *Usat* = 30 μM/s is the uptake at which the theoretical maximum of 100% FAR′max would be reached (with infinitely long stimulation). *Small dots* Theoretical receptor potential amplitudes expected for an increase of FAR′ and of membrane conductance, with the assumption of 30 pS increase per FAR′. (Modified from Kaissling 2013)

would be as many ion channels as receptor molecules (2.6×10^6 for the A-neuron of *A. polyphemus*). A number of only 1000–10,000 ion channels per A-neuron would, however, suffice in order to reach amaximum receptor potential amplitude if each ion channel contributes 30 pS (Fig. 1.5). This enormous discrepancy supports the assumption that number and size of ion channel openings may be subjected to significant reductions, for instance at high stimulus intensities (see below).

From R_{tot} and the apparent rate constant k_5 (=0.947/(s × μM) for the association of FA and R (determined by Kaissling 2009b, 2013) one obtains the average time interval needed for the ligand-receptor binding (for weak stimulation when R is about equal to R_{tot}):

$$\ln 2 / \left(R_{tot} \times k_5 \right) = 426\text{ms}$$

This time interval needed for the binding reaction of FA and R is responsible for most of the delay of the responses to single molecules observed at weak stimulus intensities. In the example of Fig. 1.3c, half of the nerve impulses were fired about 100 ms

after the end of the 1-s stimulus. Therefore, the average latency of the nerve impulses was about 600 ms. A similar average delay may be obtained from Fig. 2 of Dolzer et al. (2003) for nerve impulses recorded from antennal sensilla of *M. sexta* after weak and brief (50-ms) stimulations, using bombykal at loads below 10^{-4} µg/fp.

Several processes contribute to the latency of nerve impulses after weak pheromone stimuli:

(i) The passive transport of the stimulus molecule from the hair surface to the receptor neuron which takes about ten ms; this value results from a diffusion model, based on the measured longitudinal transport of ^{3}H-labeled pheromone along the olfactory hair (diffusion coefficient 3×10^{-7} cm^2/s, Kanaujia and Kaissling 1985). It is supported by the observed minimum delay (about 10 ms) of the receptor potential at very high stimulus intensities (Kaissling 2001, 2013).

(ii) The binding of the pheromone to the highly concentrated pheromone binding protein (PBP) within the sensillum lymph (Vogt and Riddiford 1981; see Chaps. 4, 5, 6, 7, and 8), form B. This takes about 3 ms only, for a PBP concentration of 3.8 mM (Kaissling 2009b).

(iii) The change of the complex FB to the ligand form FA able to bind to the receptor molecule, with 94 ms (ibid.).

(iv) The binding of FA and R, with the above calculated 426 ms.

(v) The change from the ligand-receptor complex FAR to the activated form FAR′, with 41 ms (ibid.).

(vi) The delay between bump onset and nerve impulse, with 10–20 ms (Fig. 1.2a–d).

The sum of these quantities fits to the observed delay of about 600 ms.

The above model reveals an apparent dissociation constant $k_{-5}/k_5 = 8.1$ µM of the ligand-receptor complex FAR. Binding experiments of Leal et al. (2005) yield a smaller dissociation constant for the complex of bombykol and PBP (form A) of 1.6 µM. This would mean that the apparent binding of the pheromone (F) to the PBP (A) is stronger than the binding of the ligand FA to the receptor molecule R. The apparent effective concentration of FA for the complex FAR′ was $EC_{50} = k_{-5}/k_5 \times k_{-6}/(k_6 + k_{-6}) = 6.8$ µM (Kaissling 2009b). This EC_{50} is close to the $EC_{50} = 1.5$ µM for bombykol and the bombykol receptor molecule expressed in *Xenopus* oocytes (Nakagawa et al. 2005).

This attempt to model pheromone reception in moths (Kaissling 2001, 2009b) is preliminary. It is based on experimental data obtained from different species of moths and types of pheromone neurons. Furthermore it does not include the sensory neuron membrane protein (SNMP). Recent work shows that this protein is involved in the interaction of pheromone, pheromone binding proteins and the OR-ORCO receptor complex (see Chap. 4). Further biochemical and physiological data are certainly needed for a more complete model of insect olfactory transduction processes.

6 Variation of ERPs

Observations of fluctuating and smooth receptor potentials suggest that the elementary receptor potentials (ERPs) may vary in shape and size. At medium stimulus intensities the receptor potential fluctuates due to superimposition of ERPs such as observed at weak stimuli (see Fig. 1.3b). With increasing stimulus intensities the fluctuations become stronger but they disappear with still higher intensities, as expected when the receptor potential amplitude approaches saturation (see Fig. 1.4).

Strikingly, pheromone derivatives with minimal modifications of the chemical structure may produce either smooth (Fig. 1.6a, second trace) or fluctuating receptor potentials (Fig. 1.6a, third trace). This is the case even if the derivatives (both about 1000-fold less effective than the pheromone) are applied at equal stimulus intensities producing similar average potential amplitudes far below saturation (Kaissling 1974). Apparently the fluctuations represent superimposed regular ERPs while the smooth response results from a larger number of smaller ERPs.

An explanation of different response types might be based on the rate constants of the ligand-receptor interaction that could differ depending on the stimulus compound (Kaissling 2009b). For instance, a given pheromone derivative could account for a smaller activation rate k_6 than the native pheromone. This would reduce the number of activations of FAR, but would not change the lifetime of FAR′ (depending on k_{-6}) and the duration of channel open state. Consequently, the derivative would produce "regular" bumps and a fluctuating response (Fig. 1.6a, third trace) as the pheromone (Fig. 1.6a, first trace). With a different derivative a larger k_{-6}, however, would reduce the number of activations per FAR complex, and shorten the lifetime of FAR′, thereby shortening also the open state of ion channels. Due to limited temporal resolution of the recording system very short events would not be visible. Many such events would add up and form a smooth overall response (Fig. 1.6a, second trace).

Important properties of olfactory neurons still cannot be explained to date, as e.g. the particular shape of the dose-response curve of moth pheromone receptor potentials covering seven $\log_{10}$ units of stimulus intensities (see Fig. 1.5). This curve reflects the need of moths to cope with an enormous range of pheromone concentrations, from those several hundred meters or even a few km downwind from the odor source up to those very close to the female pheromone gland (for references see Kaissling 1997). The measured dose-response curve of the receptor potential amplitude is much shallower than the theoretical curve (see Fig. 1.5). The theoretical curve is expected if both, FAR′ and the membrane conductance increase in linear proportion to the stimulus intensity and if the curve saturates due to a non-linear relation between conductance and voltage. The shallow shape of the measured curve suggests that number and/or size of ion channel openings are reduced with increasing stimulus intensity. Reduction of receptor potential amplitudes and associated changes of the preparation resistances occur due to adaptation after preceding strong stimuli (Zack 1979; Kaissling and Thorson 1980). The reduced sensitivity of

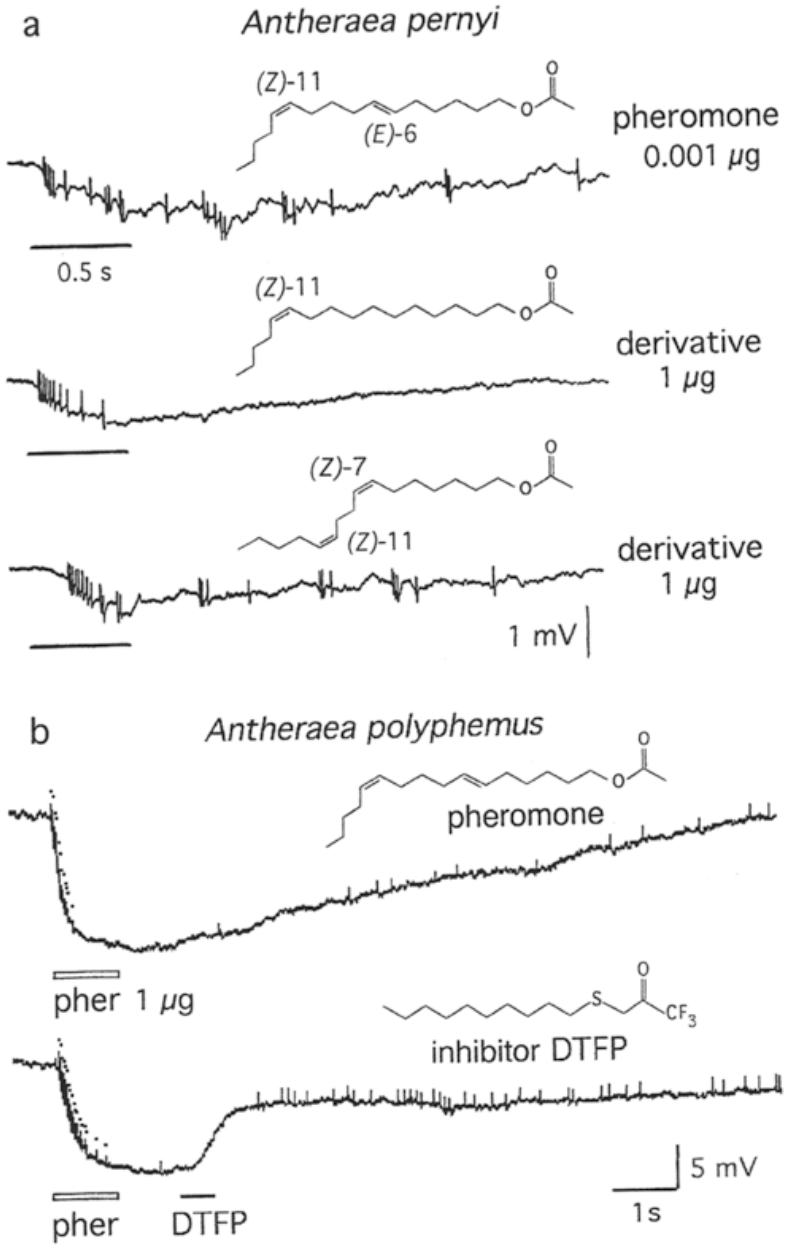

Fig. 1.6 Recordings from sensilla trichodea of saturniid moths (*Antheraea pernyi, A. polyphemus*). (**a**) *First trace:* Typical fluctuating receptor potential with irregular firing pattern of nerve impulses elicited by a weak pheromone stimulus (0.001 µg per odor source). *Second and third traces:* Responses of the same neuron upon stimulation by pheromone derivatives at 1000-fold higher load of the odor source: Smooth and fluctuating responses with regular and irregular firing, respectively (Kaissling 1977). (**b**) *Upper trace:* Strong response to a 1-s air puff with pheromone applied locally to a 400 µm hair via a capillary mouth of 40 µm diameter. The typical initial burst of nerve impulses (highlighted by dots) is followed by a silent period indicating adaptation of the impulse generator. *Lower trace:* Responses of the same neuron to the pheromone puff followed by a puff of air directed to the same locus containing decanoyl-thio-1,1,1-trifluoropropanone (DTFP). The inhibitor acts as quickly as the pheromone. The silent period of impulse firing is shortened and followed by impulse firing indicating recovery from adaptation of the impulse generator. (Modified from Pophof 1998)

the neurons appears as a substantial modification of the dose-response curves (Zack 1979; Kaissling et al. 1987; Dolzer et al. 2003).

7 Possible Mechanisms of Pheromone Response Modulation

The so-called metabotropic olfactory receptors, i.e. G-protein-coupled receptors, modulate ion channel function via intracellular second messengers (Ronnett and Moon 2002) that open ion channels from the membrane inside.

Often metabolic processes are thought to be necessary for the extreme sensitivity of olfactory neurons (Nakagawa and Vosshall 2009; Wicher et al. 2008). As discussed above, the amplification required in order to produce an ERP could be provided solely by the electrical organisation of the sensillum, i.e. by direct opening of ion channels upon binding an odorant molecule. This function, however, known for ligand-gated "ionotropic" receptors (Silbering and Benton 2010; Wicher 2015), might be performed also by "metabotropic" receptors, when stimulated at low stimulus intensities, i.e. at a few molecule hits per neuron and per s. Intracellular signal processes might rather be involved at higher stimulus intensities and cause the above-discussed shallow shape of the dose-response curve and be responsible for sensory adaptation. Here only a few aspects related to the responses to weak pheromone stimuli are discussed.

A candidate intracellular messenger is cyclic guanosine monophosphate (cGMP) since Ziegelberger et al. (1990) found an 1.34-fold increased level of cGMP in antennal homogenates of *A. polyphemus* and *B. mori* after pheromone stimuli were applied to the living antennae. In this study, no increase was found for the cyclic adenosine monophosphate (cAMP) signalling pathway. Since the authors did not detect an increase of cGMP within sensillum hairs isolated from intact antennae after 30 s pheromone stimulation they concluded that cGMP is not involved in the generation of the receptor potential but rather may modulate the nerve impulse generation within the neuron soma (Ziegelberger et al. 1990).

The latter idea is supported by whole cell-patch clamp recordings from *A. polyphemus* neurons isolated during the early phase of pupal development. Zufall et al. (1991) found that 10 µM of cGMP rapidly blocked a calcium-activated unspecific (CAN) channel. This channel is gated by 100 nM Ca^{2+}, and opens with at least four sublevels of 16 pS each and with an opening time of 1 ms. The CAN-channel, however, has not been found in the pheromone-sensitive dendrite membrane. Its function remains to be clarified.

The reports about the physiological effects of cGMP as a second messenger in moth olfactory transduction are contradictory. Patch clamp experiments using extruded dendrites of receptor neurons of *A. polyphemus* revealed pheromone-dependent channel openings of 56 pS, with opening time constants of 0.14 ms and 1.48 ms (AC1-channel; Zufall and Hatt 1991). The mean currents through this channel increased with cGMP concentrations between 1 µM up to 100 µM (with 5 mM magnesium adenosine triphosphate or MgATP).

On the contrary, receptor potentials and nerve impulse firing were substantially reduced in tip recordings when the sensillum was superfused with 100 µM of dibutyryl guanosine 3′,5′ cyclic monophosphate (db-cGMP) (Redkozubov 2000b). This membrane-permeable mimic of cGMP also diminished the bump amplitudes. Nakagawa and Touhara (2013) applied up to 100 µM doses of cGMP and cAMP to the (outer) surface of oocytes expressing the bombykol receptor BmOr-1 + BmORCO and found weak activation of currents. Responses to bombykol, however, were strongly suppressed by 100 µM doses of both cyclic nucleotides.

That second messengers play a role in moth pheromone reception is suggested by the presence of a G-protein Gq alpha subunit in moth antennae, exclusively in trichoid sensilla (Jacquin-Joly et al. 2002), and also by the effects of compounds known to interfere with the sensory transduction cascade. Further membrane-permeable compounds mimicking second messengers were extra-cellularly applied via the recording capillary electrode in contact with the opened tip of trichoid sensilla. For instance, 20 µM 1,2-dihexanoyl glycerol (DHG), mimicking diacylglycerol (DAG), a protein kinase C activator, caused impulse firing of gypsy moth neurons (Redkozubov 1996). Nerve impulses were elicited by 100 µM 1,2 dioctanoyl-sn-glycerol (DOG), another mimic of diacylglycerol, in pheromone-sensitive neurons of *A. polyphemus* (Maida et al. 2000). The above-mentioned pheromone-dependent AC1-channels of *A. polyphemus* neurons found in patch clamp studies were activated by 2.9 µM of DOG (+5 mM of MgATP, Zufall and Hatt 1991). No effects on the above AC1-channels were observed with 1 µM of inositol 1,4,5-triphosphate (IP3), another second messenger, or with 100 µM of cAMP (ibid.).

Interestingly, the G-protein activator sodium fluoride (NaF, 20 mM) elicited nerve impulse firing (Laue et al. 1997). NaF (20 mM) and DOG (100 µM) elicited bumps with impulse firing (see Fig. 1.2g) in BOL- and BAL-neurons of *B. mori* (Pophof and Van der Goes van Naters 2002). This activity was not blocked by the putative pheromone competitor DTFP (see below), suggesting that NaF and DOG tackled a stage of the transduction cascade later than the pheromone-receptor interaction. These activators elicited bumps with average amplitudes as high as those of pheromone-induced bumps (ibid.). Further studies of intracellular mechanisms involved in insect olfactory transduction are reviewed in Stengl (2017) and Wicher and Grosse-Wilde (2017).

8 Effects on the ERP by Blocking Agents and Pheromone Derivatives

Terpene compounds like geraniol or (±)-linalool (produced by plants) are known to effectively block pheromone receptor neurons in moths (Schneider et al. 1964; Den Otter et al. 1980; Kaissling et al. 1989). The NaF- or DOG-induced activity has been blocked by chemicals such as (±)-linalool or heptanol (Pophof and Van der Goes van

Naters 2002). (±)-Linalool is, however, a potent stimulant for another type of neuron in the female *B. mori* (Heinbockel and Kaissling 1996; Barrozo and Kaissling 2002). Notably there are compounds producing both excitation and inhibition, but with different time course. For instance, a stimulus with iodobenzene initially inhibits the spontaneous activity of the benzoic acid olfactory receptor neuron of the female *B. mori.* After ceasing the odor stimulus, the inhibition rapidly disappears and a transient excitation appears (De Brito-Sanchez and Kaissling 2005).

The receptor potential may be selectively blocked by decanoyl-thio-1,1,1-trifluoropropanone (DTFP, Pophof 1998), a compound known as esterase enzyme blocker (Vogt et al. 1985). This compound applied within an air puff immediately repolarised the receptor potential elicited by a preceding pheromone stimulus, without impairing the nerve impulse firing (Fig. 1.6b). DTFP strongly reduced the frequency but not the amplitudes of ERPs upon pheromone stimuli. It blocked various pheromone receptor neurons but did not act on neurons tuned to other compounds (Pophof et al. 2000). Probably this blocker with a structure similar to the one of moth pheromones competes with binding of the pheromone to the receptor molecules. The amount of (^{3}H-labeled) DTFP adsorbed on the antennal hairs causing full inhibition was similar to the calculated number of receptor molecules. DTFP strongly binds to the abundant pheromone binding protein (PBP) within the sensillum lymph. PBP is about 300-fold higher concentrated than the applied DTFP (Pophof et al. 2000). Probably the inhibitory effect is due to the binding of the DTFP-PBP complex – rather than of the free DTFP – to the receptor (ibid.). In this case PBP would binds the DTFP as rapidly as it binds the pheromone, because the inhibitory effect starts within a few ms (Fig. 1.6b). DTFP and similar compounds selectively affecting pheromone reception are discussed as tools for insect pest control (Renou et al. 2004).

9 Smooth Responses in Non-pheromone Neurons

Many types of less sensitive olfactory neurons do not show ERPs or fluctuating receptor potentials, even though they innervate sensilla morphologically similar to those housing pheromone receptor neurons. One typical example is a neuron of the female *B. mori* most sensitive to benzoic acid that produces a just detectable increase in impulse firing at 7×10^8 molecules of benzoic acid per ml of air, at an air speed of 60 cm/s (Ziesmann et al. 2000). This concentration is in the range of the human detection threshold for a few most potent odorants (Devos et al. 1990). With this threshold stimulus the benzoic acid neuron receives more than 1000 odorant molecules per second. The smooth receptor potentials of these neurons must be due to minute openings of many ion channels. Another case of mass effects of stimulus compounds are the CO_2-receptor neurons, that are extremely sensitive while responding to fractions of the natural CO_2 concentration in air but are certainly not “interested” in detecting single stimulus molecules (Stange and Rowe 1999; Jones 2013).

It remains to be shown whether the mechanism producing ERPs and nerve impulses upon single stimulus molecules is unique to pheromone sensing in moths or whether it occurs also in other insects. Particularly insects with very small-sized antennae and/or sensilla – accordingly less efficient in collecting molecules – are expected to have neurons able to detect single odorant molecules. For instance the antenna of a *Drosophila* (fruitfly) has an outline area 10,000-fold smaller than the one of a saturniid moth comb-like antenna and bears hair sensilla of 10-µm length. Of course a small efficiency of catching molecules may to some degree be compensated by a low rate of spontaneous nerve impulse firing of the neurons (Kaissling 2009a).

10 Elementary Responses of Insect Photoreceptor Cells

Finally, it should be noted that insect photoreceptor cells show elementary potential waves with amplitudes of 0.5–2.5 mV and with 30–40 ms half-width (Scholes 1965; Kirschfeld 1966; Lillywhite 1977). These waves, also called "bumps", are generated by light-sensitive channels (transient receptor potential "TRP" and TRP-like channels). They started after light flashes containing single or a few photons per cell, with latencies of 20–150 ms in the locust, and about 20 ms in the fly. The bumps could reflect single photon absorptions. In *Drosophila* (fruitfly) an average bump of 10 pA corresponds to *ca* 15 simultaneously open channels at the peak of the bump (Henderson et al. 2000).

11 Elementary Responses in Vertebrate Olfactory Neurons

There is little doubt that also in certain vertebrate olfactory neurons single molecules are sufficient to elicit nerve impulses. Dogs with 10^9 olfactory neurons per nose respond behaviorally to a concentration in air of butyric acid of 9×10^3 molecules/ml (Neuhaus 1953) or to alpha-ionone of 4×10^5 molecules/ml (Moulton 1977). With a sniff volume of 100 ml a dog would inhale 9×10^5 molecules of butyric acid. Only a fraction of the inhaled molecules would reach the olfactory epithelium. For butyric acid the number of molecules hitting the sensory neurons (9×10^5) would be at least 1000-fold smaller than the number of olfactory neurons per nose (10^9). According to Poisson statistics one million of the olfactory neurons will receive one molecule only. About 500 neurons would receive two molecules, and less than one neuron a triple hit.

Patch clamp studies in isolated vertebrate olfactory neurons showed channel openings eliciting nerve impulses in salamander (Trotier and MacLeod 1987), mouse (Maue and Dionne 1987), frog (*Rana esculenta/ridibunda*; Frings and Lindemann 1988) and rat olfactory neurons (Lynch and Barry 1989). The channel openings observed in these studies were typical square-shaped, bimodal (open/

closed) events – conducting currents of about 2 pA. In rat, the conductance of a channel was estimated to be 29 pS, a single nerve impulse was fired 20 ms or more after channel opening (ibid.).

These ion channels correspond to those described here for insect pheromone receptor neurons where amplitudes of 1 pA (or 0.3 mV) or more triggered nerve impulse firing (see Fig. 1.1e, f). The similarities between the described channel openings in vertebrates and insect ERPs/ERCs might indicate direct channel gating in an extremely vast repertoire of olfactory systems.

Other work on vertebrate olfactory neurons, mainly in amphibians, shows a different type of current waves, reminiscent of the "bumps" recorded from vertebrate photoreceptor cells, which are thought to reflect intracellular signalling processes. These responses were recorded from isolated olfactory neurons upon brief odor stimuli in salamander ("quantal-like current fluctuations"; Menini et al. 1995) and in frog ("unitary responses" of *Rana pipiens*; Bhandawat et al. 2005, 2010). In both cases the responses appeared as single current waves starting 100–400 ms after stimulus onset, reached a peak about 500 ms after stimulus onset, and returned exhibiting a half width of about 500 ms.

The "quantal" current waves with amplitudes of 0.3–1 pA were considered as presumably triggered by single odorant molecules (Menini et al. 1995), an interpretation challenged by Lowe and Gold (1995). In frog (*R. pipiens*) the wave amplitudes varied between 0.3 and 9.5 pA, with an average of 2.9 pA (Bhandawat et al. 2005). A further investigation (Bhandawat et al. 2010) showed the same wave shape at stimuli of 20–200 ms with wave amplitudes up to about 40 pA. A current wave of 1.2 pA elicited nerve impulse firing and was composed of about 35 events of 0.034 pA, each of which was thought to represent one odorant-induced channel opening.

Bhandawat et al. (2005) tried to estimate the residence (dwell) time Tc of an odorant molecule bound to the receptor molecule from the peak amplitudes of the unitary responses related to the stimulus duration. This relation was measured at very strong odorant stimulation (2 mM of cineol) thought to saturate odorant binding of the receptor molecules. At low Ca^{2+} (100 nM), the relation was linear for stimuli between 25 and 50 ms. If linearly extrapolated to zero response, the time-intercept was near zero or, not discernible, at a very small value of stimulus duration. The authors concluded that "the receptor-odorant complexes … lasted <1 ms", and considered 1 ms as the residence time Tc, a figure since then widely used in the literature discussing specifically about odorant-olfactory receptor interaction (e.g. in Kaupp 2010). Whether the approach used by the authors is suited to determine the residence time Tc – without any evidence about the three rate constants determining Tc (see above) – needs to be verified. One severe difficulty of this approach is that the estimate of Tc is based on the wave peaks occurring not until about 500 ms after stimulation.

12 Concluding Remarks

This review is an attempt to stimulate further research on the in vivo responses of olfactory neurons to single pheromone molecules, which may be recorded relatively easily from the tips of insect olfactory sensilla. The study of such responses might be helpful not only for understanding the recognition of the odorant by the OR-ORCO complex, but also for unravelling extracellular interactions of the odorant with other important proteins such as odorant (pheromone) binding proteins (OBPs, PBPs), sensory neuron membrane proteins (SNMPs), odorant degrading enzymes (ODEs) (Vogt et al. 1985; Vogt 2003, 2005; see Chaps. 4 and 5), and calmodulin (Mukunda et al. 2014). Studies of these interactions by using smallest stimulus intensities would avoid interference by sensory adaptation processes and intracellular signaling processes occuring at higher stimulus intensities. Recordings from single insect sensilla with identified olfactory neurons are more than ever crucial in studying the neurobiological basis of odor sensing. Via the recording capillary electrode at the opened hair tip, experimental drugs may conveniently be applied directly to the odorant-sensitive dendrites inside the hair shaft (see Fig. 1.1) (Kaissling 1974, 1995; Kaissling et al. 1991). This way also chemicals used for insect pest control could be tested (e.g. Kaissling 1980) and might certainly help elaborate new strategies, targeting the basic mechanism of insect olfaction.

Acknowledgement The author is grateful to Wynand M. van der Goes van Naters, Cardiff, and Uwe Koch, Kaiserslautern, for valuable suggestions and comments to earlier versions of the manuscript. Special thanks are directed to Jean-François Picimbon, Jinan, for most thoughtful editing.

References

Ala-Laurila P, Donner K, Koskelainen A (2004) Thermal activation and photoactivation of visual pigments. Biophys J 86:3653–3662

Barrozo RB, Kaissling KE (2002) Repetitive stimulation of olfactory receptor cells in female silkmoths *Bombyx mori* L. J Insect Physiol 48:825–834

Bhandawat V, Reisert J, Yau KW (2005) Elementary response of olfactory receptor neurons to odorants. Science 308:1931–1934

Bhandawat V, Reisert J, Yau KW (2010) Signaling by olfactory receptor neurons near threshold. Proc Natl Acad Sci U S A 107:18682–18687

Boeckh J, Boeckh V (1979) Threshold and odor specificity of pheromone-sensitive neurons in the deutocerebrum of *Antheraea pernyi* and *A. polyphemus* (Saturnidae). J Comp Physiol 132:235–242

Butenandt A, Beckmann R, Stamm D, Hecker E (1959) Über den Sexuallockstoff des Seidenspinners *Bombyx mori*. Reindarstellung und Konstitution. Z Naturforsch 14b:283–284

De Brito-Sanchez MG, Kaissling KE (2005) Inhibitory and excitatory effects of iodobenzene on the antennal benzoic acid receptor cell of the female silk moth *Bombyx mori* L. Chem Senses 30:1–8

De Kramer JJ (1985) The electrical circuitry of an olfactory sensillum in *Antheraea polyphemus*. J Neurosci 5:2484–24935

De Kramer JJ, Kaissling KE, Keil T (1984) Passive electrical properties of insect sensilla may produce the biphasic shape of spikes. Chem Senses 8:289–295

Den Otter CJ, Behan M, Maes FW (1980) Single cell responses in female *Pieris brassicae* (Lepidoptera: Pieridae) to plant volatiles and conspecific egg odours. J Insect Physiol 26:465–472

Devos M, Patte J, Rouault J, Laffort P, Van Gemert LJ (1990) Standardized human olfactory thresholds. Oxford University Press, Oxford, p 176

Dolzer J, Fischer K, Stengl M (2003) Adaptation in pheromone-sensitive trichoid sensilla of the hawkmoth *Manduca sexta*. J Exp Biol 206:1575–1588

Dratz EA, Hargrave PA (1983) The structure of rhodopsin and the rod outer segment disk membrane. Trends Biochem Sci 8:128

Frings S, Lindemann B (1988) Odorant response of isolated olfactory receptor cells is blocked by amiloride. J Membrane Biol 105:233–243

Gawalek P, Stengl M (2018) The Diacylglycerol Analogs OAG and DOG Differentially Affect Primary Events of Pheromone Transduction in the Hawkmoth Manduca sexta in a Zeitgebertime-Dependent Manner Apparently Targeting TRP Channels. Front Cell Neurosci 12:218. https://doi.org/10.3389/fncel.2018.00218

Gnatzy W, Mohren W, Steinbrecht RA (1984) Pheromone receptors in *Bombyx mori* and *Antheraea pernyi* II. Morphometric analysis. Cell Tissue Res 235:35–42

Heinbockel T, Kaissling KE (1996) Variability of olfactory receptor neuron responses of female silkmoths (*Bombyx mori* L.) to benzoic acid and (+)-linalool. J Insect Physiol 42:565–578

Henderson SR, Reuss H, Hardie RC (2000) Single photon responses in *Drosophila* photoreceptors and their regulation by Ca2+. J Physiol 524:179–194

Hille B (2001) Ion channels of excitable membranes, 3rd edn. Sinauer Associates, Sunderland.

Hopf TA, Morinaga S, Ihara S, Touhara K, Marks DS, Benton R (2015) Amino acid coevolution reveals three-dimensional structure and functional domains of insect odorant receptors. Nat Commun 6:6077

Jacquin-Joly E, Francois MC, Burnet M, Lucas P, Bourrat F, Maida R (2002) Expression pattern in the antennae of the newly isolated lepidopteran Gq protein alpha subunit cDNA. Eur J Biochem 269:2133–2142

Jin X, Ha TS, Smith DP (2008) SNMP is a signaling component required for pheromone sensitivity in *Drosophila*. Proc Natl Acad Sci U S A 105:10995–11000

Jones W (2013) Olfactory carbon dioxide detection by insects and other animals. Mol Cells 35:87–92

Jones PL, Pask GM, Rinker DC, Zwiebel LJ (2011) Functional agonism of insect odorant receptor ion channels. Proc Natl Acad Sci U S A 108:8821–8825

Kaissling KE (1971) Insect olfaction. In: Beidler LM (ed) Handbook of sensory physiology IV, 1. Springer, Heidelberg, pp 351–431

Kaissling KE (1974) Sensory transduction in insect olfactory receptors. In: Jaenicke L (ed) 25. Mosbacher Coll Ges Biolog Chemie, biochemistry of sensory functions. Springer, Berlin/Heidelberg/New York, pp 243–273

Kaissling KE (1977) Structures of odour molecules and multiple activities of receptor cells. In: Le Magnen J, MacLeod P (eds) Olfaction and taste VI. Inf. Retrieval, London, pp 9–16

Kaissling KE (1980) Action of chemicals, including (+)trans Permethrin and DDT, on insect olfactory receptors. In: Insect neurobiology and pesticide action (Neurotox 79). Soc Chem Industry, London, pp 351–358

Kaissling KE (1986) Chemo-electrical transduction in insect olfactory receptors. Ann Rev Neurosci 9:21–45

Kaissling KE (1987) In: Colbow K (ed) RH Wright lectures on insect olfaction. Simon Fraser University, Burnaby, p 190

Kaissling KE (1995) Single unit and electroantennogram recordings in insect olfactory organs. In: Spielman AI, Brand JG (eds) Experimental cell biology of taste and olfaction: current techniques and protocols. CRC Press, Boca Raton/New York/Tokyo, pp 361–386

Kaissling KE (1997) Pheromone-controlled anemotaxis in moths. In: Lehrer M (ed) Orientation and communication in arthropods. Birkhaeuser, Basel, pp 343–374
Kaissling KE (1998) Flux detectors versus concentration detectors: two types of chemoreceptors. Chem Senses 23:99–111
Kaissling KE (2001) Olfactory perireceptor and receptor events in moths: a kinetic model. Chem Senses 26:125–150
Kaissling KE (2009a) The sensitivity of the insect nose: the example of *Bombyx mori*. In: Marco S, Gutierrez-Galvez A (eds) Biologically inspired signal processing for chemical sensing. SCI 188. Springer, Heidelberg, pp 45–52
Kaissling KE (2009b) Olfactory perireceptor and receptor events in moths: a kinetic model revised. J Comp Physiol A 195:895–922
Kaissling KE (2013) Kinetics of olfactory responses might largely depend on the odorant-receptor interaction and the odorant deactivation postulated for flux detectors. J Comp Physiol A 199:879–896
Kaissling KE (2014) Pheromone reception in insects (the example of silk moths). In: Mucignat-Caretta C (ed) Neurobiology of chemical communication. CRC Press/Taylor & Francis, Boca Raton/London/New York, pp 99–146
Kaissling KE, Priesner E (1970) Die Riechschwelle des Seidenspinners. Naturwiss 57:23–28
Kaissling KE, Thorson J (1980) Insect olfactory sensilla: structural, chemical and electrical aspects of the functional organisation. In: Satelle DB, Hall LM, Hildebrand JG (eds) Receptors for neurotransmitters, hormones and pheromones in insects. Elsevier/North-Holland Biomedical Press, New York, pp 261–282
Kaissling KE, Kasang G, Bestmann HJ, Stransky W, Vostrowsky O (1978) A new pheromone of the silkworm moth *Bombyx mori*. Sensory pathway and behavioral effect. Naturwiss 65:382–384
Kaissling KE, Zack-Strausfeld C, Rumbo ER (1987) Adaptation processes in insect olfactory receptors. Mechanisms and behavioral significance. Olfaction and taste IX. Ann N Y Acad Sci 510:104–112
Kaissling KE, Meng LZ, Bestmann HJ (1989) Responses of bombykol receptor cells to *(Z,E)*-4,6-hexadecadiene and linalool. J Comp Physiol A 165:147–154
Kaissling KE, Keil TA, Williams L (1991) Pheromone stimulation in perfused olfactory hairs of *Antheraea polyphemus*. J Insect Physiol 37:71–78
Kanaujia S, Kaissling KE (1985) Interactions of pheromone with moth antennae: adsorption, desorption and transport. J Insect Physiol 31:71–81
Kasang G (1968) Tritium labeling of the sex attractant Bombykol. Z Naturforsch 23b:1331–1335
Kasang G, Nicholls M, von Proff L (1989a) Sex pheromone conversion and degradation in antennae of the male silkworm moth *Bombyx mori* L. Experientia 45:81–87
Kasang G, Nicholls M, Keil TA, Kanaujia S (1989b) Enzymatic conversion of sex pheromones in olfactory hairs of the male silkworm moth *Antheraea polyphemus*. Z Naturforsch 44c:920–926
Kaupp UB (2010) Olfactory signalling in vertebrates and insects: differences and commonalities. Nat Rev Neurosci 11:188–200
Keil TA (1984) Reconstruction and morphometry of silkmoth olfactory hairs: a comparative study of sensilla trichodea on the antennae of male *Antheraea polyphemus* and *Antheraea pernyi* (Insecta, Lepidoptera). Zoomorphology 104:147–156
Keil TA (1989) Fine structure of the pheromone-sensitive sensilla on the antenna of the Hawkmoth, *Manduca sexta*. Tiss Cell 21:139–151
Keil TA (1999) Morphologie and development of the peripheral olfactory organs. In: Hansson BS (ed) Insect olfaction. Springer, Berlin/Heidelberg, pp 5–47
Kirschfeld K (1966) Discrete and graded receptor potentials in the compound eye of the fly (*Musca*). In: The functional organization of the compound eye. Proceedings of the international symposium. Pergamon Press, Oxford, pp 291–307
Klein U, Keil TA (1984) Dendritic membrane from insect olfactory hairs: Isolation method and electron microscopic observations. Cell Mol Neurobiol 4:385–396

Kodadová B, Kaissling KE (1996) Effects of temperature on responses of silkmoth olfactory receptor neurones to pheromone can be simulated by modulation of resting cell membrane resistances. J Comp Physiol 179:15–27

Laue M, Maida R, Redkozubov A (1997) G-protein activation, identification and immunolocalization in pheromone-sensitive sensilla trichodea of moths. Cell Tissue Res 288:149–158

Leal WS, Chen AM, Ishida Y, Chiang VP, Erickson ML, Morgan TI, Tsuruda JM (2005) Kinetics and molecular properties of pheromone binding and release. Proc Natl Acad Sci U S A 102:5386–5391

Li Z, Ni JD, Huang J, Montell C (2014) Requirement for Drosophila SNMP1 for rapid activation and termination of pheromone-induced activity. PLoS Genet 10:e1004600. https://doi.org/10.1371/journal.pgen.1004600

Lillywhite PG (1977) Single photon signals and transduction in an insect eye. J Comp Physiol 122:189–200

Lowe G, Gold GH (1995) Olfactory transduction is intrinsically noisy. Proc Natl Acad Sci U S A 92:7864–7868

Lynch JW, Barry PH (1989) Action potentials initiated by single channels opening in a small neuron (rat olfactory receptor). Biophys J 55:755–768

Maida R, Redkozubov A, Ziegelberger G (2000) Identification of PLCß and PKC in pheromone receptor neurons of *Antheraea polyphemus*. Neuroreport 11:1773–1776

Maue RA, Dionne VE (1987) Patch-clamp studies of isolated mouse olfactory receptor neurons. J Gen Physiol 90:95–125

Menini A, Picco C, Firestein S (1995) Quantal-like current fluctuations induced by odorants in olfactory receptor cells. Nature 373:435–437

Minor AV, Kaissling KE (2003) Cell responses to single pheromone molecules may reflect the activation kinetics of olfactory receptor molecules. J Comp Physiol A 189:221–230

Moulton DG (1977) Minimum odorant concentrations detectable by the dog and their implications for olfactory receptor sensitivity. In: Müller-Schwarze D, Mozell MM (eds) Chemical signals in vertebrates. Plenum Press, New York, pp 455–464

Mukunda L, Miazzi F, Kaltofen S, Hansson BS, Wicher D (2014) Calmodulin modulates insect odorant receptor function. Cell Calcium 55:324–333

Nakagawa T, Touhara K (2013) Extracellular modulation of the silkmoth sex pheromone receptor activity by cyclic nucleotides. PLoS One 8:e63774

Nakagawa T, Vosshall LB (2009) Controversy and consensus: noncanonical signaling mechanisms in the insect olfactory system. Curr Opin Neurobiol 19:284–292

Nakagawa T, Sakurai T, Nishioka T, Touhara K (2005) Insect sex-pheromone signals mediated by specific combinations of olfactory receptors. Science 307:1638–1642

Nakagawa T, Pellegrino M, Sato K, Vosshall LB, Touhara K (2012) Amino acid residues contributing to function of the heteromeric insect olfactory receptor complex. PLoS One 7:e32372

Neher E, Sakmann B (1976) Single-channel currents recorded from membrane of denervated frog muscle fibers. Nature 260:779–802

Neuhaus W (1953) Über die Riechschärfe des Hundes für Fettsäuren. Z vergl Physiol 35:527–552

Nolte A, Funk N, Mukunda L, Gawalek P, Werckenthin A, Hansson B, Wicher D, Stengl M (2013) In situ tip-recordings found no evidence for an Orco-based ionotropic mechanism of pheromone-transduction in *Manduca sexta*. PLoS One 8:e62648

Nolte A, Gawalek P, Koerte S, Wei HY, Schumann R, Werckenthin A, Krieger J, Stengl M (2016) No evidence for ionotropic pheromone transduction in the hawkmoth *Manduca sexta*. PLoS One 11:e0166060

Pézier A, Acquistapace A, Renou M, Rospars J-P, Lucas P (2007) Ca2+ Stabilizes the Membrane Potential of Moth Olfactory Receptor Neurons at Rest and Is Essential for Their Fast Repolarization. Chem Senses 32:305–317

Pézier A, Grauso M, Acquistapace A, Monsempes C, Rospars JP, Lucas P (2010) Calcium activates a chloride conductance likely involved in olfactory receptor neuron repolarisation in the moth *Spodoptera littoralis*. J Neurosci 30:6323–6333

Pophof B (1998) Inhibitors of sensillar esterase reversibly block the responses of moth pheromone receptor cells. J Comp Physiol A 183:153–164
Pophof B, Van der Goes van Naters W (2002) Activation and inhibition of the transduction process in silkmoth olfactory receptor neurons. Chem Senses 27:435–443
Pophof B, Gebauer T, Ziegelberger G (2000) Decyl-thio-trifluoropropanone, a competitive inhibitor of moth pheromone receptors. J Comp Physiol A 186:315–323
Redkozubov A (1995) High electrical resistance of the bombykol cell in an olfactory sensillum of *Bombyx mori*: voltage- and current-clamp analysis. J Insect Physiol 41:451–455
Redkozubov A (1996) Protein kinase C is involved in the activation of receptor neurons in the olfactory sensilla of the gypsy moth. Sens Syst 10:307–312
Redkozubov A (2000a) Elementary receptor currents elicited by a single pheromone molecule exhibit quantal composition. Pfluegers Arch-Eur J Physiol 440:896–901
Redkozubov A (2000b) Guanosine 3´,5´-cyclic monophosphate reduces the response of the moth's olfactory receptor neuron to pheromone. Chem Senses 25:381–385
Renou M, Barthier A, Guerrero A (2004) Disruption of responses to pheromone by (Z)-11-hexadecenyl trifluoromethyl ketone, an analogue of the pheromone, in the cabbage army worm *Mamestra brassicae*. Pest Manag Sci 58:839–844
Rogers ME, Sun M, Lerner MR, Vogt RG (1997) Snmp-1, a novel membrane protein of olfactory neurons of the silk moth *Antheraea polyphemus* with homology to the CD36 family of membrane proteins. J Biol Chem 272:14792–14799
Rogers ME, Krieger J, Vogt RG (2001) Antennal SNMPs (sensory neuron membrane proteins) of Lepidoptera define a unique family of invertebrate CD36-like proteins. J Neurobiol 49:47–61
Ronnett GV, Moon C (2002) G proteins and olfactory signal transduction. Ann Rev 64:189–222
Sato K, Pellegrino M, Nakagawa T, Vosshall LB, Touhara K (2008) Insect olfactory receptors are heteromeric ligand-gated ion channels. Nature 452:1002–1006
Schneider D, Lacher V, Kaissling KE (1964) Die Reaktionsweise und das Reaktionsspektrum von Riechzellen bei *Antheraea pernyi* (Lepidoptera, Saturniidae). Z vergl Physiol 48:632–662
Scholes J (1965) Discontinuity of the excitation process in locust visual cells. Cold Spring Harbour Symp Quant Biol 30:517–527
Silbering AF, Benton R (2010) Ionotropic and metabotropic mechanisms in chemoreception: 'chance or design'? EMBO Rep 11:173–179
Stange G, Kaissling KE (1995) The site of action of general anaesthetics in insect olfactory receptor neurons. Chem Senses 20:421–432
Stange G, Rowe S (1999) Carbon-dioxide sensing structures in terrestrial arthropods. Micros Res Tech 47:416–427
Starrat AN, Dahm KH, Allen N, Hildebrand JG, Payne TL, Röller H (1979) Bombykal, a sex pheromone of the sphinx moth *Manduca sexta*. Z Naturforsch 34C:9–12
Steinbrecht RA, Kasang G (1972) Capture and conveyance of odour molecules in an insect olfactory receptor. In: Schneider D (ed) Olfaction and taste IV. Wiss Verlagsges, Stuttgart, pp 193–199
Stengl M, Funk NW (2013) The role of the coreceptor Orco in insect olfactory transduction. J Comp Physiol A 199:897–909
Stengl M (2017) Chemosensory transduction in arthropods. In: Byrne JH (ed) Oxford Handbooks Online. The Oxford Handbook of Invertebrate Neurobiology. Oxford University Press, pp 1–42. https://doi.org/10.1093/oxfordhb/9780190456757.013.15
Stühmer W, Roberts WM, Almers W (1985) The loose patch clamp. In: Sakmann B, Neher E (eds) Single-channel recording. Plenum Press, New York, pp 123–132
Thurm U, Küppers J (1980) Epithelial physiology of insect sensilla. In: Locke M, Smith DS (eds) Insect biology in the future. Academic, New York, pp 735–763
Trotier D, MacLeod P (1987) The amplification process in olfactory receptor cells. Ann N Y Acad Sci 510:677–679
Vermeulen A, Rospars JP (2001) Electrical circuitry of an insect olfactory sensillum. Neurocomputing 29:587–596

Vijverberg HPM, van der Zalm JM, van den Bercken J (1982) Similar mode of action of pyrethroids and DDT on sodium channel gating in myelinated nerves. Nature (Lond) 295:601–603

Vogt RG (2003) Biochemical diversity of odor detection: OBPs, ODEs and SNMPs. In: Blomquist GJ, Vogt RG (eds) Insect pheromone biochemistry and molecular biology-the biosynthesis and detection of pheromones and plant volatiles. Elsevier Academic Press, London/San Diego, pp 391–446

Vogt RG (2005) Molecular basis of pheromone detection in insects. In: Gilbert LI, Iatrou K, Gill S (eds) Comprehensive insect physiology, biochemistry, pharmacology and molecular biology, Endocrinology, vol 3. Elsevier, London, pp 753–804

Vogt RG, Riddiford LM (1981) Pheromone binding and inactivation by moth antennae. Nature (Lond) 293:161–163

Vogt RG, Riddiford LM, Prestwich GD (1985) Kinetic properties of a pheromone degrading enzyme: the sensillar esterase of *Antheraea polyphemus*. Proc Natl Acad Sci U S A 82:8827–8831

Wicher D (2015) Olfactory signaling in insects. In: Glatz R (ed) Progress in molecular biology and translational science, vol 130. Elsevier, New York, pp 37–54

Wicher D, Schaefer R, Bauernfeind R, Stensmyr MC, Heller R, Heinemann SH, Hansson BS (2008) *Drosophila* odorant receptors are both ligand-gated and cyclic-nucleotide-activated cation channels. Nature 452:1007–1011

Wicher D, Grosse-Wilde E (2017) Chemoreceptors in Evolution. In: Kaas J (ed) Evolution of Nervous Systems 2e. Elsevier, Oxford, pp 245–255

Zack C (1979) Sensory adaptation in the sex pheromone receptor cells of saturniid moths. Diss Fak Biol LMU München:1–99

Zack-Strausfeld C, Kaissling KE (1986) Localized adaptation processes in olfactory sensilla of Saturniid moths. Chem Senses 11:499–512

Ziegelberger G, Van den Berg MJ, Kaissling KE, Klumpp S, Schultz JE (1990) Cyclic nucleotide levels and guanylate cyclase activity in pheromone-sensitive antennae of the silkmoths *Antheraea polyphemus* and *Bombyx mori*. J Neurosci 10:1217–1225

Ziesmann J, Valterova I, Haberkorn K, De Brito Sanchez MG, Kaissling KE (2000) Chemicals in laboratory room air stimulate olfactory neurons of female *Bombyx mori*. Chem Senses 25:31–37

Zufall F, Hatt H (1991) Dual activation of sex pheromone-dependent ion channel from insect olfactory dendrites by protein kinase C activators and cyclic GMP. Proc Natl Acad Sci U S A 88:8520–8524

Zufall F, Hatt H, Keil TA (1991) A calcium-activated nonspecific cation channel from olfactory receptor neurons of the silkmoth *Antheraea polyphemus*. J Exp Biol 161:455–468